J Therm Anal Calorim (2012) 107:55–64
DOI 10.1007/s10973-011-1554-1

# Thermal, spectral, and thermodynamic studies for evaluation of calf thymus DNA interaction activity of some copper(II) complexes

**Mohan N. Patel · Bhupesh S. Bhatt · Promise A. Dosi**

29th STAC-ICC Conference Special Chapter


**Abstract** The square-pyramidal copper(II) complexes with ciprofloxacin (CFL) in the presence of bipyridine derivatives have been synthesized and characterized using elemental analysis, magnetic moment measurement, thermal analysis (TG), IR, mass and reflectance spectra. The thermal denaturation study has been used for evaluating calf thymus DNA interaction activity. Various spectral and hydrodynamic measurements have been used for validating the DNA interaction study. The thermodynamic profile was established for proper understanding of binding Gibbs free energy.

**Keywords** TG · DNA thermal denaturation · Nucleolytic activity · Gibbs free energy

## Introduction

Design of small molecules that are capable of binding and cleaving DNA at specific sites has been an area of considerable interest. Small molecules that bind to DNA have been used as diagnostic probes for both structural and functional aspects of nucleic acid and in the development of new therapeutic agents [1, 2]. Metal complexes that substitutionally inert, possess rich photophysical and electrochemical properties which render them as useful candidates for applications in the fields of molecular biology, biotechnology, and medicine [3]. Transition metal complexes bind to DNA by both covalent and non-covalent interactions. The three different non-covalent binding modes of interaction involves the stacking of the molecule between the base pairs of DNA, groove binding comprises the insertion of the molecule into the major or minor grooves of DNA and the electrostatic or external surface binding. Upon binding to DNA, these small molecules are stabilized through a series of weak interactions such as $\pi$-stacking interactions of aromatic heterocyclic groups and the base pairs (intercalation), hydrogen bonding, and Van der Waals interactions of functional groups bound along the groove of the DNA helix [4–7]. Various factors that govern the binding of metal complexes with DNA are shape and size of the ligand, hydrophobicity, spin state, redox potential, and hydrogen bonding ability of the complexes [8]. The emergence of diverse thermal techniques has solved many problems for estimating DNA adduct stability [9, 10].

Herein, we represent the interaction of Cu(II) ion with the second-generation quinolone, ciprofloxacin (CFL), and some bidentate ligands. More specifically, the complexes have been synthesized and characterized with, diverse analytical and spectroscopic techniques (elemental analysis, thermal analysis (TG), magnetic moment measurement, reflectance, IR, and mass spectroscopy). The potentiality of thermal techniques in investigating DNA-complex adduct stability was used along with hydrodynamic and spectral measurement for confirming the data. In continuation, we have also calculated various thermodynamic parameters for binding free energy to split the binding constant into its electrolytic and non electrolytic counterparts.

## Experimental

All the chemicals and solvents used were of reagent grade. Ciprofloxacin hydrochloride was purchased from Bayer AG (Wuppertal, Germany). Copper(II) chloride dihydrate,

M. N. Patel (✉) · B. S. Bhatt · P. A. Dosi
Department of Chemistry, Sardar Patel University, Vallabh Vidyanagar 388 120, Gujarat, India
e-mail: jeenen@gmail.com

*p*-bromo acetophenone, *p*-methyl acetophenone, *p*-chloro benzaldehyde, *p*-bromo benzaldehyde, *p*-methyl benzaldehyde, *p*-methoxy benzaldehyde, and CT DNA were purchased from Sd fine chemicals (India). Ethidium bromide and Luria Broth were purchased from Himedia (India). Acetic acid and EDTA were purchased from Sd fine chemicals (India).

## Instrumentation

IR spectra were recorded on a FT–IR Shimadzu spectrophotometer with sample prepared as KBr pellets in the range 4000–400 $cm^{-1}$. C, H, and N elemental analysis were performed on a model Perkin-Elmer 240 elemental analyzer. The metal contents of the complexes were analyzed by EDTA titration [11] after decomposing the organic matter with a mixture of $HClO_4$, $H_2SO_4$, and $HNO_3$ (1:1.5:2.5). TG was obtained with a model 5000/2960 SDTA, TA instrument (USA). The reflectance spectra were recorded on a UV-160A UV–Vis spectrophotometer, Shimadzu (Japan). The magnetic moments were measured by Gouy's method using mercury tetrathiocyanatocobaltate(II) as the calibrant ($\chi_g = 16.44 \times 10^{-6}$ cgs units at 20 °C), with a Citizen Balance. The diamagnetic correction was made using Pascal's constant. The FAB-mass spectra were recorded on a Jeol SX 120/Da-600 mass spectrometer/data system using Argon/Xenon (6 kV, 10 mA) as the FAB gas. The accelerating voltage was 10 kV and spectra were recorded at room temperature. The melting points were taken with the melting point apparatus, Adarsh Scientific Instruments (India) using mercury thermometer.

## Synthesis

Ligand $A^1$ to $A^8$ were prepared by reacting appropriate enone with pyridinium salt as reported by Neve et al. [12]. A methanolic solution of $CuCl_2{\cdot}2H_2O$ (1.5 mmol) was added to methanolic solution of bipyridines (1.5 mmol), followed by addition of a previously prepared solution of CFL (1.5 mmol) in methanol in presence of $CH_3ONa$ (1.5 mmol). The pH was adjusted at ~6.8 using dilute solution of $CH_3ONa$. Resulting solution was refluxed for 2 h on water bath, followed by concentrating it to half of its volume. A fine amorphous product of green color was obtained which was washed with ether/hexane and dried in vacuum desiccators.

## DNA binding activity

### *Electronic absorption titration*

The UV absorbance at 260 and 280 nm of the CT DNA solution in 5 mM Tris–HCl buffer (pH 7.2) gave a ratio of 1.9, indicating the DNA was free of protein [13]. The concentration of CT DNA was measured from the band intensity at 260 nm with a known $\varepsilon$ value (6600 $M^{-1}$ $cm^{-1}$) [14]. Absorption titration measurements were done by varying the concentration of CT DNA, keeping the metal complex concentration constant. The intrinsic binding constant ($K_b$) for the interaction of the complexes with CT DNA were determined from a plot of $[DNA]/(\varepsilon_a - \varepsilon_f)$ versus [DNA] using absorption spectral titration data and the following equation:

$$[DNA]/(\varepsilon_a - \varepsilon_f) = [DNA]/(\varepsilon_b - \varepsilon_f) + 1/K_b(\varepsilon_b - \varepsilon_f) \quad (1)$$

where $\varepsilon_a$, $\varepsilon_f$, and $\varepsilon_b$ correspond to $A_{obsd}$/[Cu(II) complex], the extinction coefficient for the free complex and the extinction coefficient for the complex in the fully bound form, respectively.

### *DNA-melting studies*

Thermal denaturation studies were carried out with a Perkin–Elmer Lambda-850 spectrophotometer equipped with a Peltier temperature-controlling programmer PTP-6 (±0.1 °C) in buffer. With the use of the thermal melting program, the temperature of the cell containing the cuvette was ramped from 40 to 90 °C. The absorbance at 260 nm was monitored for solutions of CT DNA (100 μM) in the absence and presence of the copper(II) complex (20 μM). The melting temperature ($T_m$) was taken as the mid-point of the hyperchromic transition.

### *Viscosity measurements*

Viscosity measurements were carried out using an Ubbelohde viscometer maintained at a constant temperature at 27.0 ± 0.1 °C in a thermostatic bath. CT DNA samples approximately 200 bp in average length were prepared by sonication in order to minimize complexities arising from DNA flexibility [15]. Flow time was measured with a digital stopwatch, and each sample was measured three times, and an average flow time was calculated. Data are presented as $(\eta/\eta_0)^{1/3}$ versus binding ratio [16], where $\eta$ is the viscosity of DNA in the presence of complex and $\eta_0$ is the viscosity of DNA alone.

## Measurements of salt dependence in DNA binding

The salt dependent equilibrium binding constant ($K_b$) of copper(II) complex to CT DNA was determined by spectrophotometric titration over the concentration range 0.005–0.100 M NaCl. A fixed amount of copper(II) complex in 0.2 M phosphate buffer at pH 7.2 and various

concentrations of NaCl was titrated with increasing amounts of DNA stock solutions. The hypochromicity and bathochromicity due to metal complex–DNA interaction was monitored by UV–Vis spectrophotometer. The $K_b$ values at various NaCl concentrations were calculated on the basis of the Eq. 1.

The salt concentration dependence of $K_b$ for the DNA binding of the copper(II) complexes was then evaluated by plotting $\ln K_b$ versus $\ln[Na^+]$ to obtain SK value, which is essential for polyelectrolyte analysis. Each measured point was the average value of at least three separate measurements with a relative standard deviation normally less than 15%.

Gel electrophoresis: photo quantization technique

For the gel electrophoresis experiments, total volume of 15 μL contain 300 μg/mL of pUC19 DNA in TE buffer (10 mM Tris, 1 mM EDTA, pH 8.0) was treated with different complexes (200 μM) and the mixture was incubated for 24 h at 37 °C in the dark. The samples were then analyzed on the base of charge and size difference on 1% agarose gel bed consisting 0.5 μg/mL of ethidium bromide at 50 V after quenching the reaction with 5 μL loading buffer (40% sucrose and 0.2% bromophenol blue). The whole bed was immersed in 1× TAE buffer (0.04 M Tris–acetate, pH 8, 0.001 M EDTA). Bands were visualized by UV light and photographed followed by estimation of intensity of the DNA bands using AlphaDigiDocTM RT. Version V.4.1.0 PC–Image software; gel documentation system.

## Result and discussion

All the complexes were analyzed using elemental analysis, magnetic measurements, reflectance, IR, and FAB-mass spectroscopy. The elemental analysis is in concurrence with proposed 1:1:1, metal:CFL:$A^n$ formulation, and theoretical expectation. The proposed reaction is shown in Scheme 1 and physical parameters are shown in Table 1.

Reflectance spectra and magnetic behavior

The electronic absorption bands of copper(II) complexes resulting from the d–d transitions are referred as ligand field or crystal field bands because their energies shift with the positions of ligands in the spectrochemical series. The reflectance spectra of the Cu(II) complexes exhibit one asymmetric broad band around 15000 $cm^{-1}$. These spectra suggest that compounds have a distorted square-pyramidal geometry of the ligands donor atoms around the $Cu^{+2}$ ion.

At room temperature, the magnetic moments of all the complexes lie in the range 1.81–1.94 B.M., which is higher

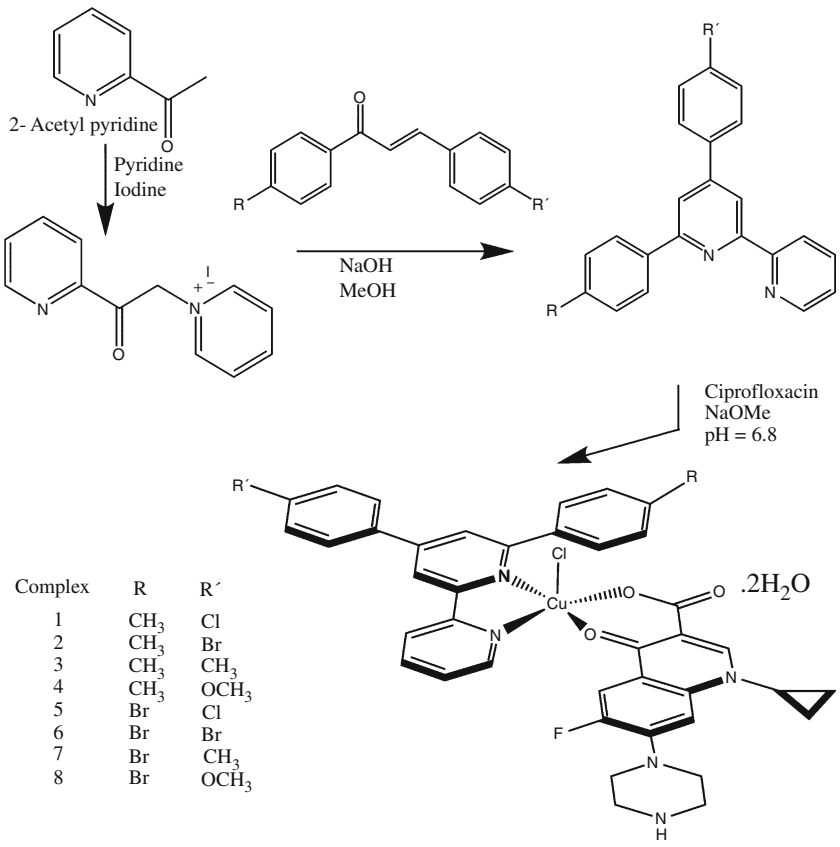


| Complex | R | R´ |
|---|---|---|
| 1 | $CH_3$ | Cl |
| 2 | $CH_3$ | Br |
| 3 | $CH_3$ | $CH_3$ |
| 4 | $CH_3$ | $OCH_3$ |
| 5 | Br | Cl |
| 6 | Br | Br |
| 7 | Br | $CH_3$ |
| 8 | Br | $OCH_3$ |

**Scheme 1** Reaction scheme for formation of complex [Cu(CFL)($A^1$)Cl] (1)

**Table 1** Physical parameters of complexes

| Complexes empirical formula | Elemental analysis/% found(required) | | | | m.p./°C | $\mu_{eff}$/B.M. |
|---|---|---|---|---|---|---|
| | C | H | N | M | | |
| $C_{40}H_{38}Cl_2FCuN_5O_5$ (1) | 58.27 (58.43) | 4.53 (4.66) | 8.70 (8.52) | 7.65 (7.73) | 236 | 1.89 |
| $C_{40}H_{38}BrClFCuN_5O_5$ (2) | 55.58 (55.43) | 4.54 (4.42) | 7.96 (8.08) | 7.26 (7.33) | 230 | 1.81 |
| $C_{41}H_{41}ClFCuN_5O_5$ (3) | 61.25 (61.42) | 4.99 (5.15) | 8.91 (8.73) | 7.82 (7.93) | 231 | 1.87 |
| $C_{41}H_{41}ClFCuN_5O_6$ (4) | 60.38 (60.22) | 4.88 (5.05) | 8.74 (8.56) | 7.71 (7.77) | 230 | 1.86 |
| $C_{39}H_{35}BrCl_2FCuN_5O_5$ (5) | 52.64 (52.80) | 4.19 (3.98) | 7.72 (7.89) | 7.09 (7.16) | 241 | 1.92 |
| $C_{39}H_{35}Br_2ClFCuN_5O_5$ (6) | 50.41 (50.28) | 3.97 (3.79) | 7.70 (7.52) | 6.71 (6.82) | 256 | 1.94 |
| $C_{40}H_{38}BrClFCuN_5O_5$ (7) | 55.32 (55.43) | 4.22 (4.42) | 8.25 (8.08) | 7.20 (7.33) | 238 | 1.83 |
| $C_{40}H_{38}BrClFCuN_5O_6$ (8) | 54.57 (54.43) | 4.46 (4.34) | 7.77 (7.93) | 7.14 (7.20) | 242 | 1.87 |

than the spin-only value of 1.73 B.M. Such divergence is not uncommon in mononuclear Cu(II) complexes due to the mixing of some angular moment from nearby excited states via spin–orbit coupling [17].

## IR spectra

The prominent IR spectral data of the complexes are shown in Table 2. The $\nu$(C=O) stretching vibration band appears at 1708 $cm^{-1}$ for CFL, while for complexes it appears at 1613–1621 $cm^{-1}$. This shift toward lower energy suggests that coordination occurs through the carbonyl oxygen of pyridine ring [18]. The strong absorption bands obtained at 1624 and 1340 $cm^{-1}$ in CFL could be assigned for $\nu$(COO) asymmetric and symmetric vibrations, respectively, while in the metal complexes, these bands are observed at 1560–1577 and 1351–1372 $cm^{-1}$. The difference $\Delta\nu = \nu(COO)_{as} - \nu(COO)_s$ is very much informative in determining the coordination mode of the ligands. If the difference is greater than 200 $cm^{-1}$, it would point toward monodentate coordination behavior of the carboxylato group [19–22] of the CFL. These data are further supported by $\nu$(M–O) [23] which appear at 509–516 $cm^{-1}$ for complexes.

In the investigated complexes, the $\nu$(C=N) band of bipyridine derivatives is observed at about 1584 $cm^{-1}$. This band shift to higher frequency at $\sim$1626 $cm^{-1}$ in complexes suggests the bidentate N–N coordination of the ligand [24, 25]. The $\nu$(M–N) band at $\sim$530–545 $cm^{-1}$ is assigned to N $\rightarrow$ M bonding of complexes [26].

## Thermal analysis

The objective of this section is to analyze the thermal behavior of the complexes having in view the composition confirmation and the water of crystallization molecule role assessment. For the complexes, the water molecule are stepwise eliminated namely the crystallization one up to 140 °C while the coordination one in 140–200 °C temperature range, both steps being endothermic [27–30]. TG has been carried out at a heating rate of 10 °C per minute in the range of 20–800 °C under $N_2$ atmosphere (Fig. 1). On interpretation of the TG curve, three distinct mass losses are observed. The first mass loss occurs between 50 and 120 °C, second between 180 and 310 °C, and finally between 320 and 620 °C. Mass lost occurring during first decomposition step corresponds to two molecules of crystallization water, where as mass loss during second step corresponds to decomposition of neutral bidentate ligand and third step corresponds to decomposition of CFL leaving behind the CuO as residue. The similar thermal

**Table 2** IR spectra data

| Complexes | $\nu$(C=O) pyridone/$cm^{-1}$ | $\nu(COO)_{as}$/$cm^{-1}$ | $\nu(COO)_s$/$cm^{-1}$ | $\Delta\nu$/$cm^{-1}$ | $\nu$(M–N)/$cm^{-1}$ | $\nu$(M–O)/$cm^{-1}$ |
|---|---|---|---|---|---|---|
| Ciprofloxacin | 1708 | 1624 | 1340 | 284 | | – |
| 1 | 1619 | 1560 | 1364 | 196 | 530 | 515 |
| 2 | 1613 | 1575 | 1372 | 203 | 547 | 506 |
| 3 | 1621 | 1577 | 1372 | 202 | 545 | 516 |
| 4 | 1618 | 1569 | 1372 | 197 | 538 | 505 |
| 5 | 1614 | 1556 | 1351 | 205 | 539 | 509 |
| 6 | 1622 | 1564 | 1368 | 196 | 544 | 507 |
| 7 | 1627 | 1567 | 1365 | 199 | 540 | 514 |
| 8 | 1616 | 1571 | 1379 | 192 | 545 | 505 |

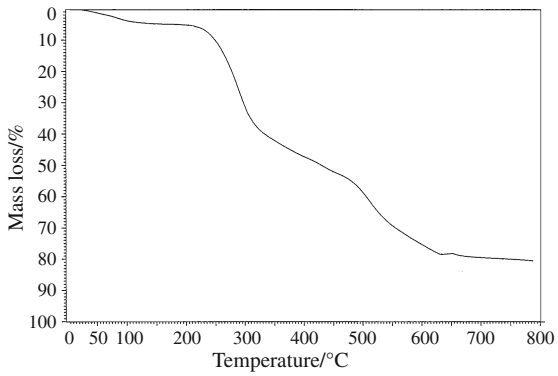


**Fig. 1** TG analysis of 1 carried out at a heating rate of 10 °C per minute in the range of 20–800 °C under $N_2$ atmosphere

degradation trend was observed and reported in the literature for quinolone metal complexes [31].

FAB-mass spectra

Figure 2 represents the FAB-mass spectrum of complex 1 that is $[Cu(CFL)(A^1)Cl]\cdot 2H_2O$, obtained using *m*-nitro benzyl alcohol as matrix. Peaks at 136, 137, 154, 289, and 307 *m/z* value are due to usage of matrix. Peaks at $m/z = 786$ and 788 in spectra are assigned to (M) and (M + 2) of complex molecule associated with $H^+$ ion in absence of lattice water. Loss of chlorine atom gave a fragment ion peak at $m/z = 749$, which also confirm that chlorine atom attached to metal ion with covalent bond. Several other fragments at 419, 393, 356, 331, and 323 *m/z* value are observed, attributed to fragments associated with matrix and different numbers of $H^+$ ions.

DNA binding activity

*Electron absorption study*

The binding of the complexes to the CT DNA has been studied by electronic absorption spectral technique. We have observed bathochromic shift along with significant hypochromicity for all complexes. The equilibrium DNA binding constants ($K_b$) determination of the complexes to CT DNA was obtained by monitoring the change of the absorption intensity of the spectral bands with increasing concentration of CT DNA.

The changes observed in the UV spectra of the complexes after mixing it with DNA indicate that the interaction of complexes with DNA takes place by a direct formation of a new complex with double-helical DNA [32]. Extent of the binding strength of complexes was quantitatively determined by calculating intrinsic binding constants $K_b$ of the complexes by monitoring the change in absorbance at various concentration of DNA. From the plot of $[DNA]/(\varepsilon_a - \varepsilon_f)$ versus [DNA] (Fig. 3), the $K_b$ value of complexes were determine and were found to be 1.27, 1.20, 1.10, 1.06, 1.85, 1.80, 1.25, and 1.28 ($\times 10^4$), respectively. These spectral characteristics are consistent with a mode of interaction that involves a stacking interaction between the complex and the base pairs of DNA, which means that the complexes can intercalate into the double-helix structure of DNA. The higher binding efficiency of the bipyridines

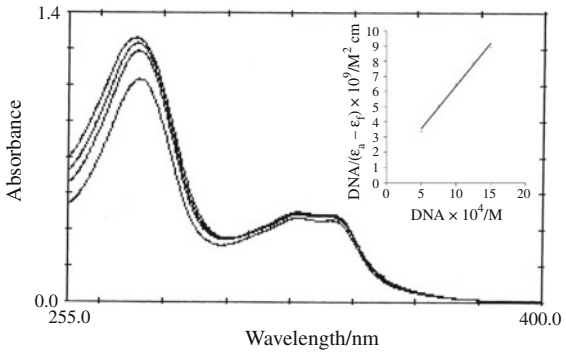


**Fig. 3** Electronic absorption titration curve of $[Cu(CFL)(A^1)Cl]$ (1) in absence and in presence of increasing amount of CT DNA in 5 mM Tris–HCl buffer (pH 7.2), [complex] = 15 μM, [DNA] = 50–150 μM with incubation period of 30 min at 37 °C, *Inset* plot of $[DNA]/(\varepsilon_a - \varepsilon_f)$ versus [DNA]

**Fig. 2** FAB-mass spectrum of 1, that is $[Cu(CFL)(A^1)Cl]$, obtained using *m*-nitro benzyl alcohol

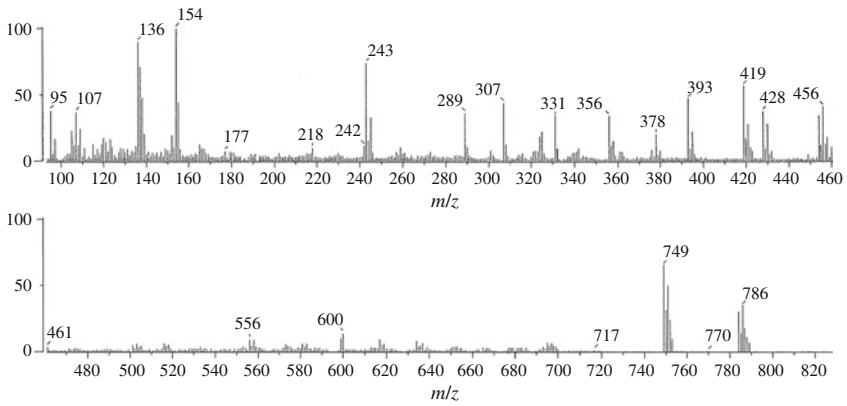

analog could be due to the presence of extended planar aromatic ring in bipyridines.

*Thermal denaturation studies*

The melting of DNA is an important parameter to study the interaction of transition metal complexes with nucleic acids. Thermal behaviors of DNA in the presence of complexes can give an insight into their conformation changes when temperature is raised, and offer information about the interaction strength of complexes with DNA. The melting temperature $T_m$, at which 50% of the DNA has become single strand, can be determined from the thermal denaturation curves of DNA by monitoring the absorption changes at 260 nm. According to the literature [33–36], the intercalation of intercalators generally results in a considerable increase in melting temperature ($T_m$). In the absence of the complex, a DNA-melting experiment showed that $T_m$ of CT DNA (100 μM) is 74.2 ± 0.1 °C under experimental conditions (Fig. 4). The observed increasing melting temperature ($\Delta T_m$) is 4.7, 4.5, 3.9, 4.1, 5.7, 5.4, 5.1, and 5.2 °C in the presence of complexes (20 μM) 1, 2, 3, 4, 5, 6, 7, and 8, respectively. The increase amount of $T_m$ is comparable to that observed for classical intercalators [33–35].

*Viscosity measurements*

Viscosity measurements were performed on DNA by varying the concentration of the compound. Hydrodynamic measurements that are sensitive to length changes are regarded as the least ambiguous and the most critical tests of a DNA binding model in solution, providing reliable evidence for the DNA binding mode [36]. Classical intercalation causes a significant increase in the viscosity of DNA solutions due to the increase in separation of base pairs at intercalation sites, which results in an increase in the overall DNA contour length. In contrast, complexes that bind exclusively in DNA grooves by means of partial and/or non-classic intercalation typically cause either a less prominent change or no change at all in DNA solution viscosity [37]. The results (Fig. 5) reveal that the compound produces an increase in the relative viscosity of CT DNA. These results indicate that the interaction involves an intercalation, with the compound binding between two adjacent base pairs. As increasing the amounts of complexes, viscosity of DNA increases steadily, which is similar to that of the classical intercalative complex $[Ru(phen)_2(DPPZ)]^{2+}$ where DPPZ is dipyrido [3,2-a:2,3-c]phenazine. The results suggest that the all title complexes intercalate between the base pairs of DNA and the binding affinity of complexes is higher than CFL but less than ethidium bromide.

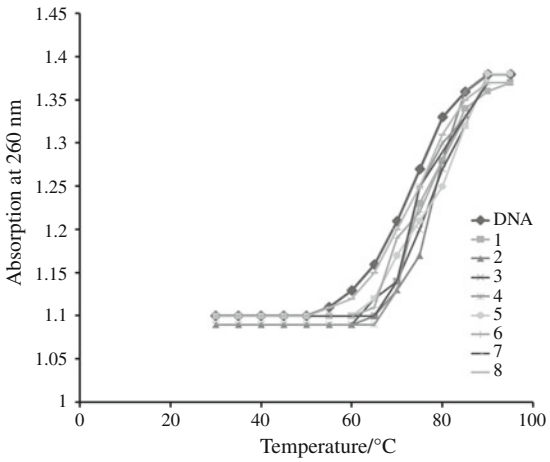


**Fig. 4** Melting curves of CT DNA in the absence and presence of 1–8

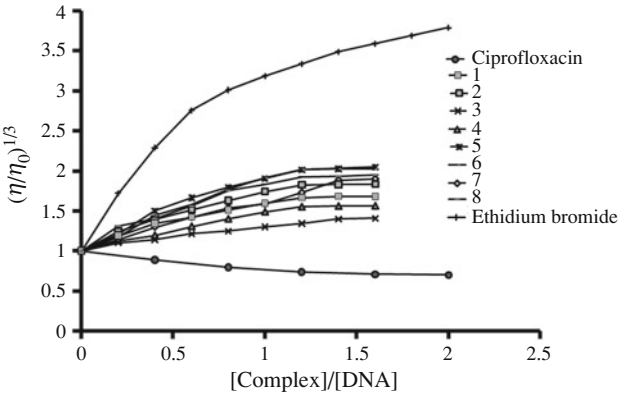


**Fig. 5** Effect on relative viscosity of DNA under the influence of increasing amount of complexes at 27 ± 0.1 °C in 5 mM Tris–HCl buffer (pH 7.2) as a medium

Salt dependence of binding constants

The typical plots of [DNA] versus [DNA]/($\varepsilon_a - \varepsilon_f$) for the determination of binding constant ($K_b$) of complex 1 to CT DNA at various concentrations of NaCl based on Eq. 1 was used (Fig. 6). The detailed results are collected in Table 3. The reported binding constants are obtained over the concentration range 0.005–0.1 M NaCl, in order to apply polyelectrolyte theory to the calculation of the non-electrostatic binding constants and separate the binding free energy change into its electrostatic and non-electrostatic contributions. The salt concentrations of 0.005–0.1 M were selected in this study, because the polyelectrolyte theories are strictly applicable to salt concentrations of lower than 0.1 M. It has been reported that the dependence of $K_b$ on salt concentration becomes non linear at higher concentrations of salt [38]. The plot of ln[$Na^+$] against ln$K_b$ for the binding of complex 1 to DNA is given in Fig. 7.

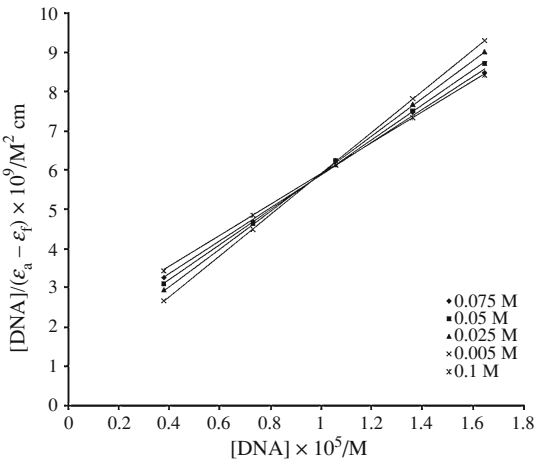


**Fig. 6** Typical plots of $[DNA]/(\varepsilon_a - \varepsilon_f)$ versus [DNA] for the spectrophotometric titration of 1 with increasing amount of [DNA] in 0.2 M phosphate buffer pH 7.2 at 25 °C and various concentrations of NaCl

**Table 3** Equilibrium binding constant ($K_b$) for the binding of 1 to CT DNA in 0.2 M phosphate buffer (pH 7.2) at 25 °C and various concentrations of NaCl

| $[Na^+]$/M | $K_b/10^3/M^{-1}$ bp | $K_t^0/10^3/M^{-1}$ bp | $K_t^0/K_b$/% |
|---|---|---|---|
| 0.005 | 11.1 | 1.0 | 8.6 |
| 0.025 | 5.9 | 1.1 | 18.9 |
| 0.050 | 4.2 | 1.1 | 26.4 |
| 0.075 | 3.1 | 1.0 | 32.1 |
| 0.100 | 2.6 | 1.0 | 36.8 |
| Average = 1.0 ± 0.08 ($10^3$) | | | |

It is clear from the plots that the binding constant decreases with increasing salt concentration. This is due to the stoichiometric amount of ion release that follows the binding of charged ligand, i.e., copper(II) complex [39], suggesting that electrostatic interaction is involved in the DNA binding event. Using the slope of linear fitting of Fig. 7, we may calculate non-electrostatic binding constant ($K_t^0$) at various concentrations of NaCl ($[Na^+]$) according to the following polyelectrolyte theory [39],

$$\ln K_b = \ln K_t^0 + Z\xi^{-1}\{\ln(\gamma_\pm \delta)\} + Z\psi \ln[Na^+]$$

where $Z\psi$ is estimated from the slope of the regression line in Fig. 7. $Z$ is partial charge on the binding ligand involved in the DNA interaction as predicted by polyelectrolyte theory, $\psi$ is the fraction of counter ions associated with each DNA phosphate unit ($\psi = 0.88$ for double-stranded B-form DNA), $\gamma_\pm$ is the mean activity coefficient at cation concentration of $Na^+$, and the remaining terms are constants for double-stranded DNA in B-form, i.e., $\xi = 4.2$ and $\delta = 0.56$. Results of the calculations are summarized in

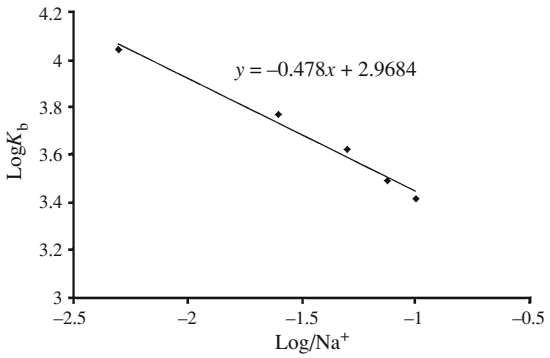


**Fig. 7** Salt dependence of binding constant ($K_b$) for the binding of 1 to CT DNA

Table 4 along with the percentage of $K_t^0$ contribution to the total binding constants ($K_b$) at various concentrations of $Na^+$. The $K_t^0$ can be taken as a measure how large the non-electrostatic forces stabilize the ligand–DNA interaction. In contrast to the $K_b$ values which are salt dependent, the magnitude of $K_t^0$ is constant throughout the concentration of NaCl employed with the average value of $1.0 \times 10^3$ $M^{-1}$ bp. This is consistent with the expectation for the salt-independency of this parameter. Although the values of $K_t^0$ are constant throughout the concentrations of salt, the percentage of $K_t^0$ contributions to the $K_b$ increases significantly and reach a maximum of 36.8% at $[Na^+] = 0.1$ M. It can be expected that at higher concentrations of salt, e.g., at physiological condition ($Na^+ \approx 0.2$ M), the non-electrostatic forces would play a major role in the DNA binding of the copper(II) complex. The value of 26.4% for the non-electrostatic binding constant found in the DNA binding of complex 1 at NaCl = 0.05 M is considered to be high even when it is compared with those of other proven intercalators such as ethidium (12.3%) at the same ionic strength [40].

Further analysis is also possible to dissect the binding free energy change ($\Delta G^0$) for the binding of complex 1 to DNA into its electrostatic ($\Delta G_{pe}^0$) and non-electrostatic ($\Delta G_t^0$) contributions at a given concentration of NaCl. Table 4 summarizes the results of energetics calculation for the binding of metal complexes to DNA in 0.05 M NaCl as well as proven organic intercalator, EtBr [39, 40]. for the purpose of comparison. The total binding free energy changes listed in Table 4 were calculated based on the standard Gibbs relation:

$$\Delta G^0 = -RT \ln[K_b]$$

where $R$ is the gas constant and $T$ is the temperature in Kelvin. The salt dependence of the binding constant is defined as the slope, $SK$. The $SK$ value can then be used to calculate the polyelectrolyte contribution of the free energy change ($\Delta G_{pe}^0$) to the overall free energy change ($\Delta G^0$) at a given NaCl concentration by the relation [39, 41]:

**Table 4** Thermodynamic parameters for the binding of copper(II) complexes to CT DNA at 0.005 M NaCl

| DNA Binders | $K_b/10^3/M^{-1}$ bp | $\Delta G^0$ | SK | $\Delta G^0_{pe}$ | $K^0_t/10^3$ $(\%K^0_t/K_b)/M^{-1}$ bp | $\Delta G^0_t(\%\Delta G^0_t/\Delta G^0)$ |
|---|---|---|---|---|---|---|
| 1 | 4.2 | −20.7 | 0.478 | −3.1 | 1.3 (32.1) | −17.6 (85.2) |
| 2 | 3.9 | −20.5 | 0.467 | −3.0 | 1.3 (32.9) | −17.5 (85.4) |
| 3 | 3.7 | −20.4 | 0.466 | −3.0 | 1.2 (33.0) | −17.4 (85.3) |
| 4 | 3.4 | −20.1 | 0.471 | −3.0 | 1.1 (32.6) | −17.1 (85.0) |
| 5 | 4.9 | −21.1 | 0.481 | −3.1 | 1.6 (31.8) | −18.0 (85.3) |
| 6 | 4.7 | −20.9 | 0.477 | −3.1 | 1.5 (32.1) | −17.9 (85.4) |
| 7 | 4.4 | −20.8 | 0.491 | −3.2 | 1.4 (31.1) | −17.2 (84.8) |
| 8 | 4.3 | −20.7 | 0.476 | −3.1 | 1.4 (32.2) | −17.7 (85.3) |
| EtBr[a] | 494 | −32.2 | 0.75 | −5.0 | 61.0 (12.3) | −27.2 (84.5) |

[a] Taken from ref. [40]

$$\Delta G^0_{pe} = (SK)RT \ln[Na^+]$$

The difference between the Gibbs free energy change ($\Delta G^0$) and $\Delta G^0_{pe}$ is defined as the non-electrostatic free energy change,

$$\Delta G^0_t = \Delta G^0 - \Delta G^0_{pe}$$

The quantity $\Delta G^0_t$ corresponds to the portion of the binding free energy change which is independent of salt concentrations and contains a minimal contribution from polyelectrolyte effects such as coupled ion release.

## Gel electrophoresis

When plasmid DNA was subjected to electrophoresis after interaction, upon illumination of gel (Fig. 8) the fastest migration was observed for super coiled (SC) Form I, where as the slowest moving was open circular (OC) Form II and the intermediate moving is the linear (L) Form III generated on cleavage of open circular. The data of plasmid cleavage are presented in Table 5. Here all the complexes show the higher cleavage ability. The different DNA-cleavage efficiency of the complexes, metal salt, and drugs is due to the difference in binding affinity of the complexes to DNA and the structural dissimilarities of ligands [42].

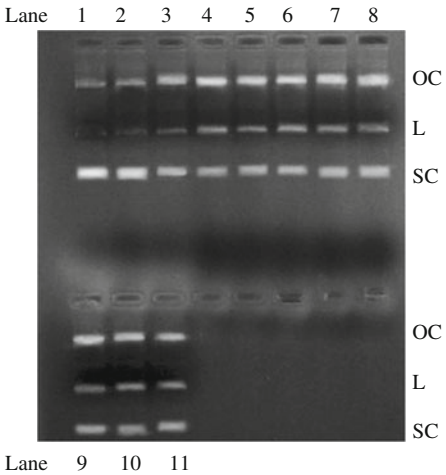


**Fig. 8** Photogenic view of interaction of pUC19 DNA (300 μg/mL) with series of copper(II) complexes (200 μM): *Lane 1* DNA control, *Lane 2* $CuCl_2{\cdot}2H_2O$, *Lane 3* CFL, *Lane 4* [Cu(CFL)($A^1$)Cl] (1), *Lane 5* [Cu(CFL)($A^2$)Cl] (2), *Lane 6* [Cu($A^3$)(CFL)Cl] (3), *Lane 7* [Cu(CFL)($A^4$)Cl] (4), *Lane 8* [Cu(CFL)($A^5$)Cl] (5), *Lane 9* [Cu($A^6$)(CFL)Cl] (6), *Lane 10* [Cu(CFL)($A^7$)Cl] (7), *Lane 11* [Cu(CFL)($A^8$)Cl] (8)

**Table 5** Gel electrophoretic data

| Compounds | % SC | % OC | % L | % Cleavage |
|---|---|---|---|---|
| DNA Control | 79 | – | 21 | |
| DNA + Metal salt | 77 | – | 23 | 2.53 |
| DNA + CFLH | 48 | 15 | 37 | 39.21 |
| DNA + 1 | 28 | 27 | 45 | 64.55 |
| DNA + 2 | 29 | 30 | 41 | 63.29 |
| DNA + 3 | 30 | 26 | 44 | 62.02 |
| DNA + 4 | 30 | 28 | 42 | 62.02 |
| DNA + 5 | 24 | 28 | 48 | 69.62 |
| DNA + 6 | 25 | 35 | 40 | 68.35 |
| DNA + 7 | 27 | 26 | 47 | 65.82 |
| DNA + 8 | 26 | 32 | 42 | 67.08 |

## Conclusions

The thermal study shows presence of two water of crystallization molecules. The increase in melting point of DNA–metal complex adduct than DNA in thermal denaturation study suggest higher DNA interaction strength of metal complexes. The Data of DNA thermal denaturation study are well supported by viscosity measurement, UV–Vis absorption spectroscopy, and gel electrophoresis. The viscometry data suggests classical intercalation for all the complexes. The bathochromicity and hypochromicity

observed in UV–Vis absorption curve for DNA binding experiment is consistent for classical intercalation mode of binding. The gel electrophoresis experiment again validate sufficient interaction between DNA and Cu(II) complexes. The thermodynamic profile of complex–DNA interaction is illustrated as binding free energy by absorption data. The effect of increasing salt concentration is clearly visualized and suggests electrostatic interaction existence in presence of electrolytic material.

## References


1. Bhattacharya PK, Barton JK. Influence of intervening mismatches on long-range guanine oxidation in DNA duplexes. J Am Chem Soc. 2001;123:8649–56.
2. Delaney S, Yoo J, Stemp EDA, Barton JK. Charge equilibration between two distinct sites in double helical DNA. Proc Natl Acad Sci. 2004;101:10511–6.
3. Rajski SR, Williams RM. DNA cross-linking agents as antitumor drugs. Chem Rev. 1998;98:2723–96.
4. Zhang QL, Liu JG, Xu H, Li H, Liu JZ, Zhou H, Qu LH, Ji LN. Synthesis, characterization and DNA-binding studies of cobalt(III) polypyridyl complexes. Polyhedron. 2001;20:3049–55.
5. Das S, Kumar GS. Molecular aspects on the interaction of phenosafranine to deoxyribonucleic acid: model for intercalative drug–DNA binding. J Mol Struc. 2008;872:56–63.
6. Nafisi S, Manouchehri F, Riahi HAT, Varavipour M. Structural features of DNA interaction with caffeine and theophylline. J Mol Struc. 2008;875:392–9.
7. Kornilova SV, Miskovsky P, Tomkova A, Kapinos LE, Hackl EV, Andrushchenko VV, Grigoriev DN, Blagoi YP. Vibrational spectroscopic studies of the divalent metal ion effect on DNA structural transitions. J Mol Struc. 1997;408:219–23.
8. Ng CH, Ong HKA, Kong CW, Tan KW, Rahman RN, Yamin BM, Ng SW. Factors affecting the nucleolytic cleavage of DNA by (N, N′-ethylenendiaminediacetato)metal(II) complexes, M(edda). Crystal structure of Co(edda). Polyhedron. 2006;25:3118–26.
9. Zuzzi S, Onori G, Cametti C. Thermal stability of DNA in DNA–induced dotap liposome aggregates. J Therm Anal Calorim. 2008;93(2):527–33.
10. Khvedelidze M, Mdzinarashvili T, Partskhaladze T, Nafee N, Schaefer UF, Lehr CM, Schneider M. Calorimetric and spectrophotometric investigation of PLGA nanoparticles and their complex with DNA. J Therm Anal Calorim. 2010;99:337–48.
11. Vogel AI. Textbook of quantitative inorganic analysis. 4th ed. London: ELBS and Longman; 1978.
12. Neve F, Crispini A, Campagna S, Serroni S. Synthesis, structure, photophysical properties, and redox behavior of cyclometalated complexes of iridium(III) with functionalized 2,2′-bipyridines. Inorg Chem. 1999;38:2250–8.
13. Marmur J. A procedure for the isolation of deoxyribonucleic acid from micro-organisms. J Mol Biol. 1961;3:208–18.
14. Reichmann ME, Rice SA, Thomas CA, Doty P. A further examination of the molecular weight and size of desoxypentose nucleic acid. J Am Chem Soc. 1954;76:3047–53.
15. Chaires JB, Dattagupta N, Crothers DM. Studies on interaction of anthracycline antibiotics and deoxyribonucleic acid: equilibrium binding studies on the interaction of daunomycin with deoxyribonucleic acid. Biochemistry. 1982;21:3933–40.
16. Cohen G, Eisenberg H. Viscosity and sedimentation study of sonicated DNA–proflavine complexes. Biopolymers. 1969;8:45–55.
17. Figgis BN, Lewis J, Wilkins RG. Modern coordination chemistry: principles and methods. New York: Willey Interscience; 1960.
18. Leban I, Turel I, Bukovec N. Synthesis, characterization, and crystal structure of a copper(II) complex with quinolone family member (ciprofloxacin): bis(1)-cyclopropyl-6-fluoro-1,4-dihydro-4-oxo-7-piperazin-1ylquinoline-3-carboxylate) copper(II) chloride hexahydrate. J Inorg Biochem. 1994;56:273–82.
19. Nakamoto K. Infrared and Raman spectra of inorganic and coordination compounds. New York: Wiley Interscience; 1986.
20. Anacona JR, Rodriguez I. Synthesis and antibacterial activity of cephalexin metal complexes. J Coord Chem. 2004;57:1263–9.
21. Deacon GB, Philips RJ. Relationships between the carbon-oxygen stretching frequencies of carboxylato complexes and the type of carboxylate coordination. Coord Chem Rev. 1980;33:227–50.
22. Chohan ZH, Suparan CT, Scozzafava A. Metal binding and antibacterial activity of ciprofloxacin complexes. J Enzym Inhib Med Chem. 2005;20:303–7.
23. Turel I, Leban I, Bukovec N. Crystal structure and characterization of the bismuth(III) compound with quinolone family member (ciprofloxacin). Antibacterial study. J Inorg Biochem. 1997;66:241–5.
24. Patel SH, Pansuriya PB, Chhasatia MR, Parekh HM, Patel MN. Coordination chain polymeric assemblies of trivalent lanthanides with multidentate Schiff base. Synthetic, spectral investigation and thermal aspects. J Therm Anal Calorim. 2008;91(2):413–8.
25. Parekh HM, Panchal PK, Patel MN. Transition metal(ii) ions with dinegative tetradentate Schiff base. J Therm Anal Calorim. 2006;86(3):803–7.
26. Freedman HH. Intramolecular H-bonds. I. A spectroscopic study of the hydrogen bond between hydroxyl and nitrogen. J Am Chem Soc. 1961;83:2900–5.
27. Badea M, Olar R, Marinescu D, Uivarosi V, Nicolescu TO, Iacob D. Thermal study of some new quinolone ruthenium(III) complexes with potential cytostatic activity. J Therm Anal Calorim. 2010;99:829–34.
28. Ababei LV, Kriza A, Musuc AM, Andronescu C, Rogozea EA. Thermal behaviour and spectroscopic studies of complexes of some divalent transitional metals with 2-benzoil-pyridilizonicotinoylhydrazone. J Therm Anal Calorim. 2010;101:987–96.
29. Kose DA, Gokce G, Gokce S, Uzun I. Bis(*N*,*N*-diethylnicotinamide) *p*-chlorobenzoate complexes of Ni(II), Zn(II) and Cd(II):Synthesis and characterization. J Therm Anal Calorim. 2009;95:247–51.
30. Dziewulska-Kułaczkowska A. Manganese(II), cobalt(II), nickel(II), copper(II) and zinc(II) complexes with 4-oxo-4H–1-benzopyran-3-carboxaldehyde. Thermal, spectroscopic and magnetic characterization. J Therm Anal Calorim. 2010;101:1019–26.
31. Zupancic M, Cerc Korosec R, Bukovec P. The thermal stability of ciprofloxacin complexes with magnesium(II), zinc(II) and cobalt(II). J Therm Anal Calorim. 2001;63:787–95.
32. El–Metwaly NM. Spectral and biological investigation of 5-hydroxyl-3-oxopyrazoline 1-carbothiohydrazide and its transition metal complexes. Trans Met Chem. 2007;32:88–94.
33. Waring MJ. Complex formation between ethidium bromide and nucleic acids. J Mol Biol. 1965;13:269.
34. Kelly JM, Tossi AB, McConell DJ, OhUigin C. A study of the interactions of some polypyridylruthenium(II) complexes with DNA using fluorescence spectroscopy, topoisomerisation and thermal denaturation. Nucleic Acids Res. 1985;13:6017–34.
35. Neyhart GA, Grover N, Smith SR, Kalsbeck WA, Fairly TA, Cory M, Thorp HH. Binding and kinetics studies of oxidation of DNA by oxoruthenium(IV). J Am Chem Soc. 1993;115:4423–8.
36. Wheate NJ, Brodie CR, Collins JG, Kemp S, Aldrich-Wright JR. DNA intercalators in cancer therapy: organic and inorganic drugs and their spectroscopic tools of analysis. Mini Rev Med Chem. 2007;7:627–48.

37. Hertzberg RP, Dervan PB. Cleavage of double helical DNA by methidium-propyl-EDTA-iron(II). J Am Chem Soc. 1982;104: 313–5.
38. Haq I, Lincoln P, Suh D, Norden D, Chowdhry BZ, Chaires JB. Interaction of DELTA- and LAMBDA-[Ru(phen)2DPPZ]2+ with DNA: a calorimetric and equilibrium binding study. J Am Chem Soc. 1995;117:4788–96.
39. Mudasir, Wijaya K, Yoshioka N, Inoue H. DNA binding of iron(II) complexes with 1,10-phenanthroline and 4,7-diphenyl-1, 10-phenanthroline: salt effect, ligand substituent effect, base pair specificity and binding strength. J Inorg Biochem. 2003;94:263–71.
40. Satyanarayana S, Dabrowiak JC, Chaires JB. Neither DELTA- nor LAMBDA-tris(phenanthroline)ruthenium(II) binds to DNA by classical intercalation. Biochemistry. 1992;31:9319–24.
41. Chaires B, Satyanarayana S, Suh D, Fokt I, Przewloka T, Priebe W. Parsing the free energy of anthracycline antibiotic binding to DNA. Biochemistry. 1996;35:2047–53.
42. Sigman DS, Graham DR, Marshall LE, Reich KA. Cleavage of DNA by coordination complexes. Superoxide formation in the oxidation of 1,10-phenanthroline-cuprous complexes by oxygen—relevance to DNA—cleavage reaction. J Am Chem Soc. 1980;102:5419–21.